Acta Pharmacologica Sinica

www.nature.com/aps

ARTICLE

Blueberry-derived exosomes-like nanoparticles ameliorate nonalcoholic fatty liver disease by attenuating mitochondrial oxidative stress

Wan-jun Zhao[1], Yang-ping Bian[1], Qiu-hui Wang[1], Fei Yin[1,2], Li Yin[1,2], Yong-lan Zhang[1,2] and Jian-hui Liu[1,2]

Accumulating evidence indicates that mitochondrial dysfunction and oxidative stress play a pivotal role in the initiation and progression of nonalcoholic fatty liver disease (NAFLD). In this study, we found that blueberry-derived exosomes-like nanoparticles (BELNs) could ameliorate oxidative stress in rotenone-induced HepG2 cells and high-fat diet (HFD)-fed C57BL/6 mice. Preincubation with BELNs decreased the level of reactive oxygen species (ROS), increased the mitochondrial membrane potential, and prevented cell apoptosis by inducing the expression of Bcl-2 and heme oxygenase-1 (HO-1) and decreasing the content of Bax in rotenone-treated HepG2 cells. We also found that preincubation with BELNs accelerated the translocation of Nrf2, an important transcription factor of antioxidative proteins, from the cytoplasm to the nucleus in rotenone-treated HepG2 cells. Moreover, administration of BELNs improved insulin resistance, ameliorated the dysfunction of hepatocytes, and regulated the expression of detoxifying/antioxidant genes by affecting the distribution of Nrf2 in the cytoplasm and nucleus of hepatocytes of HFD-fed mice. Furthermore, BELNs supplementation prevented the formation of vacuoles and attenuated the accumulation of lipid droplets by inhibiting the expression of fatty acid synthase (FAS) and acetyl-CoA carboxylase 1 (ACC1), the two key transcription factors for de novo lipogenesis in the liver of HFD-fed mice. These findings suggested that BELNs can be used for the treatment of NAFLD because of their antioxidative activity.

Keywords: blueberry-derived exosomes-like nanoparticles (BELNs); de novo lipogenesis; mitochondria; nonalcoholic fatty liver disease (NAFLD); oxidative stress

Acta Pharmacologica Sinica (2022) 43:645–658; https://doi.org/10.1038/s41401-021-00681-w

INTRODUCTION

Nonalcoholic fatty liver disease (NAFLD) is the most common chronic liver disease worldwide and is emerging as a serious clinical and social problem due to its prevalence among obese individuals [1, 2]. Accumulating evidence from epidemiology and high-fat diet-induced animal models reveals that chronic excessive energy intake is one of the major causes of NAFLD, which increases the accumulation of fat (especially triglycerides) and induces oxidative stress, lipid peroxidation, and inflammation in hepatocytes [3, 4].

Mitochondrial dysfunction and oxidative stress play a pivotal role in the initiation and progression of NAFLD [5]. As a key player in fat metabolism and energy production, mitochondria can restrain fat accumulation in hepatocytes by increasing the β-oxidation of fatty acids [6]. Unfortunately, mitochondria-mediated fatty acid β-oxidation is usually abolished in NAFLD, and the development of NAFLD is accompanied by a pro-oxidative state and mitochondrial-induced reactive oxygen species (ROS) production, which ultimately leads to hepatocyte damage and apoptosis by altering associated cellular signaling cascades [7–9]. Recent evidence shows that alterations in mitochondrial dysfunction and oxidative stress can contribute to the development and progression of NAFLD by modifying the production of excess ROS, the mitochondrial unfolded protein response, mitophagy, and mitochondrial biogenesis [10–12].

Blueberry is a flowering plant that belongs to the Ericaceae family and contains polyphenols, anthocyanins, and flavonoids shows antioxidant, anti-inflammatory, and antitumor activities, and improves metabolic function and cognitive performance [13–16]. Blueberry polyphenols were shown to prevent alcoholic fatty liver disease in C57BL/6J mice by promoting autophagy to accelerate lipolysis and attenuate the accumulation of triglycerides (TGs) in hepatocytes [17]. Most importantly, blueberry juice supplementation has been found to prevent CCl_4-induced hepatic fibrosis by reducing hepatocyte injury and lipid peroxidation, elevating the expression of metallothionein and superoxide dismutase (SOD) activity, reducing oxidative stress, and decreasing the protein levels of alpha-smooth muscle actin and collagen type III in the liver [18, 19]. However, elucidating the mechanisms underlying these beneficial effects and the active components associated with the mechanisms is needed.

In this study, we screened blueberry-derived exosomes-like nanoparticles (BELNs) and found they could attenuate the oxidative stress induced by rotenone in human HepG2 cells and

[1]Chongqing Key Lab of Medicinal Chemistry & Molecular Pharmacology, Chongqing University of Technology, Chongqing 400054, China and [2]College of Pharmacy and Bioengineering, Chongqing University of Technology, Chongqing 400054, China
Correspondence: Fei Yin (fyin@cqut.edu.cn) or Jian-hui Liu (jhliu@cqut.edu.cn)

Received: 23 January 2021 Accepted: 13 April 2021
Published online: 14 May 2021

HFD-fed C57BL/6 mice. Our data indicated that preincubation with BELNs decreased the level of ROS, increased the mitochondrial membrane potential, prevented cell apoptosis by increasing the expression of antiapoptotic proteins such as Bcl-2 and heme oxygenase-1 (HO-1), affecting the distribution of nuclear factor erythroid 2-related factor 2 (Nrf2), and decreasing the Bax protein level in rotenone-treated HepG2 cells. We also found that administration of BELNs improved insulin resistance, regulated the expression of detoxifying/antioxidant genes by mediating the activation of Nrf2, ameliorated liver dysfunction, prevented vacuole formation, and attenuated the accumulation of lipid droplets in the livers of HFD-fed mice.

MATERIALS AND METHODS

Materials

Rotenone, 2,6-di-tert-butyl-4-methylphenol (BHT), PEG8000, and JC-1 were obtained from Sigma (St Louis, MO, USA). Nrf2 (SC-722), Bcl-2 (SC-56015), HO-1 (SC-390091), Bax (SC-20067), and β-actin (SC-58673) antibodies were purchased from Santa Cruz (Dallas, TX, USA). iScript cDNA synthesis kits (1708891) were purchased from Bio-Rad (Hercules, CA, USA). CM-H2DCFA and DiO (3,3′-dioctadecyloxacarbocyanine perchlorate) fluorescent probes, DAPI, TUNEL Apoptosis Detection Kit (C1088), MitoTracker Green (C1048), and other chemicals were purchased from Beyotime (Shanghai, China). A DiR (1,1′-dioctadecyl-3,3,3′,3′-tetramethylindotricarbocyanine iodide) fluorescent probe (D9111) was obtained from Bioss (Beijing, China). A normal chow diet (NCD, 1022) and a high-fat diet (HFD, D12451, Research Diets) were purchased from Ruishi Biotech (Shanghai, China).

Isolation of blueberry-derived exosome-like nanoparticles

Fourteen edible plants, *Vaccinium corymbosum* (blueberry), *Cucumis sativus* Linn. (cucumber), *Dioscoreae Rhizoma* (Chinese yam), *Momordica charantia* Linn. (bitter gourd), *Amygdalus persica* Linn. (peach), *Zizyphus jujuba* (red dates), *Lactuca sativa* Linn. var. *ramosa Hort* (lettuce), *Allium sativum* Linn. (garlic), *Actinidia chinensis* Planch, *Lonicera japonica* Thunb, *Forsythia suspensa*, *Glycyrrhiza uralensis* Fisch, *Lilium brownii* var. *viridulum Baker*, and *Salvia miltiorrhiza*, were purchased from a local supermarket for this study. The plants with abundant juice (blueberry, cucumber, yam, bitter gourd, and peach) were milled and directly extracted with an electric blender, and the other less juicy plants were ground and extracted in a twofold volume of distilled water (liquid:solid ratio, mL/g). The mixtures were filtered once with gauze, and the collected juice was sequentially centrifuged at $1000 \times g$ for 10 min, $3000 \times g$ for 20 min, $10{,}000 \times g$ for 30 min at 4 °C in an Eppendorf centrifuge (5910R, Eppendorf, CA, USA) to remove large particles and cellular debris. The supernatant was filtered with a 1.0 μm membrane filter (Millipore, MA, USA), and the solution was incubated with 8% PEG8000 (Catalog No. 89510, Sigma) overnight and then centrifuged at $10{,}000 \times g$ for 30 min to obtain exosomes-like nanoparticles (ELNs). ELNs were weighed and resuspended in PBS (Supplementary Fig. S1a). For each experiment, the ELNs were freshly prepared and diluted with sterile PBS.

Cell culture

Human hepatoblastoma HepG2 cells were purchased from the China Center for Type Culture Collection (Wuhan, China) and routinely maintained in a humidified incubator with a 5% CO_2 atmosphere. The medium was low glucose Dulbecco's modified Eagle's medium supplemented with 10% (*v/v*) fetal bovine serum, 100 U/mL penicillin, and 100 μg/mL, which was changed every other day.

Characterization of BELNs

For observation of the morphology of BELNs, freshly prepared BELNs (5 μL) were stained with 5 μL of uranyl acetate for 1 min and spotted onto a glow-discharged, carbon-coated Formvar grid. The morphology of the BELNs was observed with transmission electron microscopy (Hitachi 7500, Tokyo, Japan). All images were captured at a voltage of 80 kV. The particle size and surface zeta potential of the BELNs in aqueous solution (0.1 mg/mL) were determined by dynamic light scattering at 25 °C using a NanoBrook Omni Particles Size Analyzer (Brookhaven Instruments Co., USA).

Increasing evidence indicates that exosomes are phospholipid bilayer vesicles that can deliver rich cargo (protein, RNA, and lipids) in a natural pathway for genetic material transfer within organisms, even between unrelated species [20, 21]. To characterize the components of BELNs, we evaluated the protein, RNA, and lipids of BELNs with polyacrylamide gel electrophoresis (PAGE), agarose gel electrophoresis, and thin-layer chromatography (TLC), respectively. Generally, RNAs from BELNs were extracted with a miRNeasy Mini kit (Qiagen, MD, USA) and separated on an agarose gel. Proteins were extracted from BELNs using RIPA cell lysis buffer (Beyotime, Shanghai, China), run on a Bis-Tris protein gel, and visualized with Coomassie brilliant blue staining. Lipids from BELNs were purified using the Folch method [22], loaded on a silica gel TLC plate, separated using a chloroform/methanol/acetic acid mixture (190:9:1), and stained with 10% $CuSO_4$ in 8% phosphoric acid solution.

Screening of antioxidative ELNs

Hydrogen peroxide (H_2O_2) has been widely used to mimic oxidative stress in vitro [23, 24]. In this study, the antioxidative activity of ELNs was evaluated by determining the cell viability in H_2O_2-treated HepG2 cells with a 3-(4,5-dimethylthiazol-2-yl)-2,5-diphenyltetrazolium bromide (MTT) colorimetric assay. In brief, HepG2 cells were added to 24-well plates (3×10^4 cells/well) and cultured overnight. The cells were pretreated with 100 μg/mL ELNs or the same volume of PBS for 4 h and then stimulated with 400 μM H_2O_2 for 24 h. The cells were incubated with MTT (0.5 mg/mL final concentration) for 4 h at 37 °C. The formazan crystals were dissolved with dimethyl sulfoxide (DMSO), and the absorbance was measured with a microplate reader (Tecan, NC, USA) using a reference wavelength of 630 nm and a test wavelength of 570 nm.

Uptake of BELNs by HepG2 cells

After BELNs were incubated with 5 μM DiO (a widely used lipophilic tracer that is weakly fluorescent in water but highly fluorescent and quite photostable when incorporated into membranes) for 30 min, the mixture was centrifuged at $100{,}000 \times g$ at 4 °C for 30 min. The DiO-labeled BELNs were resuspended in PBS, filtered with a 0.22 μm membrane (Millipore, MA, USA) and then added to the media of HepG2 cells. The uptake of BELNs was observed and imaged by E-C2 confocal microscopy (Nikon, Tokyo, Japan) at 0, 1.5, 3, or 6 h. Cellular nuclei were stained with DAPI.

Determination of ROS

Rotenone can dose-dependently induce mitochondria-mediated apoptosis and the generation of ROS in human liver HepG2 cells [25]. For evaluation of the antioxidative activity of BELNs, intracellular ROS in rotenone-treated HepG2 cells was first examined using the fluorescent molecular probe CM-H2DCFA, which was dissolved in DMSO as a concentrate. Briefly, HepG2 cells were plated in a six-well plate at 1×10^5 cells/well and cultured overnight. The cells were preincubated with 50, 100, or 200 μg/mL BELNs or 20 μM BHT (a positive control in this study) for 4 h. Then, 2 μM rotenone was added and incubated for another 24 h. Then, the cells were incubated with 25 μM CM-H2DCFDA in serum-free medium for 30 min at 37 °C and washed once with PBS. The fluorescence intensity was determined with a microplate reader (Tecan, Sunrise, USA) with excitation at 485 nm and emission at 530 nm, and the pictures were imaged with fluorescence microscopy (Nikon, Tokyo, Japan).

Measurement of mitochondrial membrane potential

The effect of BELNs on the mitochondrial membrane potential in rotenone-treated HepG2 cells was determined using a JC-1 fluorescent probe according to the suggestions from the supplier (Beyotime, Shanghai, China). In brief, after HepG2 cells were preincubated with 50, 100, or 200 μg/mL BELNs or 20 μM BHT for 4 h, 2 μM rotenone was added and incubated for another 24 h. After that, the cell culture medium was aspirated, and the cells were incubated with 10 μg/mL JC-1 for 20 min at 37 °C. JC-1 solution was aspirated, and the cells were rinsed three times with cell culture medium and imaged with fluorescence microscopy (Nikon, Tokyo, Japan) at Ex/Em = 514 nm/529 nm for JC-1 monomeric dye (green) and Ex/Em = 585 nm/590 nm for the aggregate form of JC-1 (red). Similarly, the fluorescence intensity was determined with a microplate reader (Tecan, NC, USA).

TUNEL staining

In this study, the cellular apoptosis induced by rotenone in HepG2 cells was evaluated by TUNEL (TdT-mediated dUTP nick end labeling) staining according to the guidelines from the supplier (Beyotime, Shanghai, China). Generally, after HepG2 cells were treated with 2 μM rotenone in the presence or absence of BELNs, the cells were fixed with 4% fresh polyoxymethylene for 30 min, washed once with PBS, permeabilized with 0.3% Triton X-100 for 5 min at room temperature, and washed twice with PBS. The cells were incubated with 0.3% H_2O_2 in PBS at room temperature for 20 min to inactivate endogenous peroxidase. The TdT enzyme was incubated with digoxigenin-labeled dUTP at 37 °C for 1 h. After the enzymatic reaction was terminated, the cells were incubated with streptavidin-HRP-labeled secondary antibody for 30 min, washed three times with PBS, and then stained with DAB chromogenic solution for 30 min at room temperature. The results were visualized, and images were captured with a confocal microscope (Nikon, Tokyo, Japan).

Animals

All animal experiments were approved by the Animal Ethical and Welfare Committee of Chongqing University of Technology, and all procedures involved in the animal experiments were carried out following the principles and guidelines of the Chinese Council Animal Care. Male C57BL/6 mice (6–8 weeks) were obtained from Tengxin Biotechnology Co. (Chongqing, China) and allowed ad libitum access to food and water unless otherwise stated, and rooms were maintained at 22 °C and 50% humidity on a 12-h light/dark cycle. Fifty mice were randomly divided into five groups (ten in each group); the mice in one group were fed a normal chow diet (NCD), and those in the other four groups were fed a high-fat diet (HFD). After 8 weeks, the mice in three HFD groups were administered BELNs (intragastric administration, once every other day) at 25, 50, or 100 mg/kg for a continued 4 weeks. All the animals were weighed once every other day. Before dissection, the mice were euthanized by CO_2 inhalation. The levels of TGs, total cholesterol (TC), high-density lipoprotein cholesterol (HDL-C), low-density lipoprotein cholesterol (LDL-C), aspartate aminotransferase (AST), and alanine aminotransferase (ALT) in serum were measured using a Vitros-250 Chemistry Analyzer (Johnson & Johnson, New Brunswick, NJ, USA).

Glucose tolerance test

The glucose tolerance test was performed at the 12th week of experimental feeding as previously described. Generally, after C57BL/6 mice were fed BELNs for 4 weeks, the mice were fasted overnight (12 h), 2.5 g/kg glucose was administered intragastrically, blood samples were collected from the tail vein at 0, 30, 60, and 120 min, and the blood glucose level was determined with a One Touch Ultra Mini Blood Glucose Monitoring System (Johnson, Life Scan, Inc., Milpitas, CA, USA).

Measurement of SOD, GSH, and MDA activities

Liver samples were homogenized in a buffer (0.25 mol/L sucrose, 0.5 mmol/L ethylenediaminetetraacetic acids (EDTA), 50 mmol/L HEPES, protease inhibitors, and phosphatase inhibitors) and incubated for 30 min on ice. The homogenate was centrifuged at 1500 × *g* for 10 min at 4 °C. The supernatant was used to measure the contents of superoxide dismutase (SOD), glutathione (GSH), and malondialdehyde (MDA) with commercial assay kits (Nanjing Jiancheng Bioengineering Institute, Nanjing, China) according to the manufacturer's protocol. SOD activity was measured at 550 nm, GSH levels were analyzed at 420 nm, and MDA levels were determined at 532 nm using a microplate reader (Tecan, NC, USA).

Immunohistochemistry

After the mice were administered BELNs for 4 weeks (intragastric administration, once every other day), the livers were isolated and fixed (10% formalin solution in 0.1 M PBS), frozen at −80 °C overnight, and cut into 10 μm sections on a freezing microtome (Leica, Nussloch, Germany). The sections were permeabilized in 0.1% Triton X-100 in PBS and blocked in 1% BSA in PBS before incubation with the primary antibody. Then, the samples were stained with Nrf2 antibody (SC-722, Santa Cruz, Dallas, TX, USA) together with DAPI (Invitrogen, CA, USA). Fluorescence images were acquired using a confocal microscope (Nikon, Tokyo, Japan).

Protein extraction

After the liver tissues or rotenone-treated cells were washed once with ice-cold PBS, whole-cell extracts were obtained by using modified RIPA buffer in the presence of 1% protease/phosphatase inhibitor cocktail, and the protein concentrations were measured with a BCA protein assay kit from Beyotime (Shanghai, China).

For preparation of the cytosolic and nuclear fractions, the cells or tissues were homogenized in cold buffer A (20 mM HEPES pH 7.5, 0.15 mM EDTA, 10 mM KCl, 20 mM NaF, 0.5 mM dithiothreitol, 1 mM sodium orthovanadate, 1% NP-40, and protease inhibitors). The homogenate was incubated on ice for 30 min and then centrifuged at 10,000 × *g* for 10 min at 4 °C. The supernatant corresponding to the cytosolic fraction was immediately frozen at −80 °C for further experiments. The nuclear pellet was resuspended in cold buffer B (20 mM HEPES pH 8.0, 0.1 mM EDTA, 20 mM NaF, 1 mM sodium orthovanadate, 0.4 M NaCl, 0.2 mM dithiothreitol, and protease inhibitor) and incubated for 30 min on ice. Nuclear debris was removed by centrifugation at 12,000 × *g* for 10 min at 4 °C. The supernatants corresponded to the nuclear fraction. The proteins were quantified with a BCA protein assay kit from Beyotime (Shanghai, China). Western blotting was performed to determine the expression of Nrf2 in the cytoplasm and nucleus.

Western blot

Equal amounts of proteins (20–30 μg) were separated by 10% SDS-PAGE and electrotransferred to a PVDF membrane (Immobilon P; Millipore, MA, USA), and the membranes were then blocked for 2 h at room temperature with 5% skim milk in TBST (20 mM Tris, 150 mM NaCl, 2.7 mM KCl, 0.1% Tween 20, pH 7.4). The membranes were incubated with primary antibodies against Bcl-2, Bax, HO-1, Nrf2, or β-actin (Santa Cruz, Dallas, TX, USA) at dilutions of 1:500 to 1:2000 overnight at 4 °C, followed by incubation with HRP-conjugated secondary antibody. Excess antibody was washed off with TBST, and the protein bands were visualized with ECL Western blotting reagent (Millipore, MA, USA). Signal bands were quantified by densitometric analysis using ImageJ software (available from NIH at http://imagej.nih.gov/ij/) after scanning the blotted membrane. Three independent experiments were performed for each condition.

Statistical analysis

All data are presented as the mean ± standard deviation. Statistical differences between groups were analyzed using one-way ANOVA

with Dunnett's multiple comparisons test, and a two-tailed, unpaired Student's *t* test was performed for comparison of two groups. $P < 0.05$ was considered to represent a significant difference. Statistical analysis was performed with GraphPad Prism 8.01 software (La Jolla, CA, USA).

RESULTS

Screening and characterization of blueberry-derived exosomes-like nanoparticles

In this study, we collected and screened fourteen edible plant-derived exosome-like nanoparticles (the detailed description of the edible plants and the protocol for exosome-like nanoparticle isolation are shown in Supplementary Fig. S1a). The results from the MTT assay indicated that BELNs significantly increased cell viability in H_2O_2-treated human HepG2 hepatocytes (Fig. S1b).

Before evaluating the antioxidative activity in vitro, we first determined the size distribution and surface zeta potential of the BELNs with a NanoBrook Omni Particles Size Analyzer (Brookhaven Instruments Co., NY, USA). The results showed that the size of the BELNs was in the range of 150–250 nm, with a mean diameter of 189.62 nm (Fig. 1a). The zeta potential was −2.52 mV (Fig. 1b). Transmission electron microscopy analysis revealed that the BELNs appeared as individual exosome-like nanoparticles with sphere-shaped morphology (Fig. 1c). Exosomes usually contain RNAs, proteins, and lipids [26]. In this study, the agarose gel results showed that RNAs existed in the BELNs, and most of them were small-sized RNAs (Fig. 1d). The results from PAGE demonstrated that the mass weight of BELN proteins ranged from 10 to 250 kDa (Fig. 1e). TLC analysis revealed that the BELNs contained a series of lipids (Fig. 1f). All these results demonstrated that the BELNs used in this study appeared to have exosome-like characteristics and contained RNAs, proteins, and lipids.

Then, we observed the uptake of BELNs labeled with DiO (a widely used lipophilic tracer that is weakly fluorescent in water but highly fluorescent and photostable when incorporated into membranes) in HepG2 cells. The results indicated that the BELNs could be taken up by HepG2 cells in a time-dependent manner (Fig. 1g).

Rotenone is a well-known inducer of ROS that inhibits electron transfer from complex I to the ubiquinone chain and blocks oxidative phosphorylation [25]. Therefore, in the present study, a rotenone-induced cell model in HepG2 human hepatoblastoma cells was used to evaluate antioxidative activity. The results from the MTT assay showed that the BELNs had no evident effect on HepG2 cell viability in the range of 50–200 μg/mL (Fig. 1h), and preincubation with BELNs alleviated the cytotoxicity of rotenone by increasing HepG2 cell viability in a dose-dependent manner. Pretreatment with 200 μg/mL BELNs for 4 h increased the cell viability from 69% to 88% in the 2 μM rotenone-treated HepG2 cells (Fig. 1i).

BELNs attenuated the oxidative stress induced by rotenone in HepG2 cells

Mitochondria are the main organelles for energy generation through oxidative phosphorylation in eukaryotic cells, and mitochondrial membrane potential (MMP) is the major driving force [27]. We first determined the effect of the BELNs on the content of mitochondria and the production of ROS. As expected, the BELNs significantly increased the content of mitochondria (Fig. 2a) and inhibited the production of ROS in a dose-dependent manner in the rotenone-treated HepG2 cells (Fig. 2b and c). Furthermore, JC-1 staining revealed a significant reduction in MMP in the rotenone-treated HepG2 cells, but preincubation with BELNs effectively prevented the effect of rotenone on HepG2 cells (Fig. 2d–g).

BELNs inhibited rotenone-induced cell apoptosis

To explore whether the BELNs increased cell viability by attenuating cell apoptosis, we measured the expression of apoptosis-associated proteins, including Bcl-2, Bax, and HO-1, by Western blots in the rotenone-treated HepG2 cells. The results indicated that treatment with rotenone significantly decreased the protein levels of Bcl-2 and HO-1 but increased the Bax protein level in HepG2 cells. Similar to 2,6-di-tert-butyl-4-methylphenol (BHT, a common antioxidant, which was used as a positive control in this study), preincubation with the BELNs dose-dependently prevented the effects of rotenone on the protein levels of Bcl-2, Bax, and HO-1 in HepG2 cells (Fig. 3a–e). TUNEL staining confirmed that pretreatment with BELNs strongly attenuated the cell apoptosis induced by rotenone in HepG2 cells (Fig. 3f).

Increasing evidence indicates that Nrf2 is a crucial transcription factor and induces the expression of a range of antioxidant enzymes and/or proteins by translocating from the cytoplasm to the nucleus in mammalian cells challenged by oxidative stress [28]. To explore the molecular mechanisms underlying BELN-mediated prevention of cell apoptosis induced by rotenone, we determined the distribution of Nrf2 in the cytoplasm and nucleus in the rotenone-treated HepG2 cells. The Western blot results demonstrated that treatment with rotenone evidently decreased the content of Nrf2 in the nucleus but increased the Nrf2 content in the cytoplasm of HepG2 cells, but preincubation with BELNs significantly prevented the effect of rotenone on the distribution of Nrf2 and accelerated the translocation of Nrf2 from the cytoplasm to the nucleus in HepG2 cells (Fig. 3g–j).

BELNs improved insulin resistance in the HFD-fed mice

Before exploring the effect of the BELNs on the HFD-fed mice, we observed the uptake and distribution of DiR-labeled BELNs after intragastric administration. The results showed that BELNs could be taken up by C57BL/6 mice and quickly distributed into several organelles, including the small intestine, liver, and spleen (Fig. 4a). Then, we evaluated the effects of the BELNs on the HFD-fed mice, and the data revealed that although administration of BELNs (25, 50, or 100 mg/mouse, once every other day, administered intragastrically) for 4 weeks (at the beginning of the 8th week) had no significant effect on body weight (Fig. 4b–d) or food intake (Fig. 4e), BELN supplementation apparently improved insulin resistance (Fig. 4f–h) and decreased fasting glucose (Fig. 4i) and insulin content (Fig. 4j) in the serum of the HFD-fed mice, suggesting that administration of BELNs might be beneficial for improving the pathological features of NAFLD.

BELNs improved liver dysfunction in the HFD-fed mice

H&E staining demonstrated that there were many vacuoles in the liver of the HFD-fed mice, but BELN supplementation dramatically prevented this phenomenon. Oil red staining revealed that administration of the BELNs also significantly attenuated the accumulation of lipid droplets in the liver (Fig. 5a) and the liver weight (Fig. 5b) in the HFD-fed mice. To explore the mechanisms by which the BELNs prevent the accumulation of lipid droplets, we determined the effects of the BELNs on the expression of fatty acid synthase (FAS) and acetyl-CoA carboxylase 1 (ACC1), two key genes associated with fatty acid biosynthesis. The qRT-PCR results demonstrated that the BELNs decreased the mRNA levels of FAS and ACC1 in the livers of the HFD-fed mice (Fig. 5c and d).

Furthermore, we observed that administration of the BELNs distinctively decreased the contents of TC (Fig. 6a) and TGs (Fig. 6b), the levels of ALT (Fig. 6c) and AST (Fig. 6d), and the content of LDL-C (Fig. 6e) and increased the content of HDL-C (Fig. 6f) in the HFD-fed mice. All these data suggested that BELNs might be beneficial for liver dysfunction in the HFD-fed mice.

BELNs attenuated oxidative stress and regulated the expression of apoptosis-associated proteins in the liver of the HFD-fed mice

Many studies have shown that oxidative stress plays a pivotal role in the development of NAFLD [29]. In this study, we determined the activities of antioxidative enzymes in the livers of HFD-fed

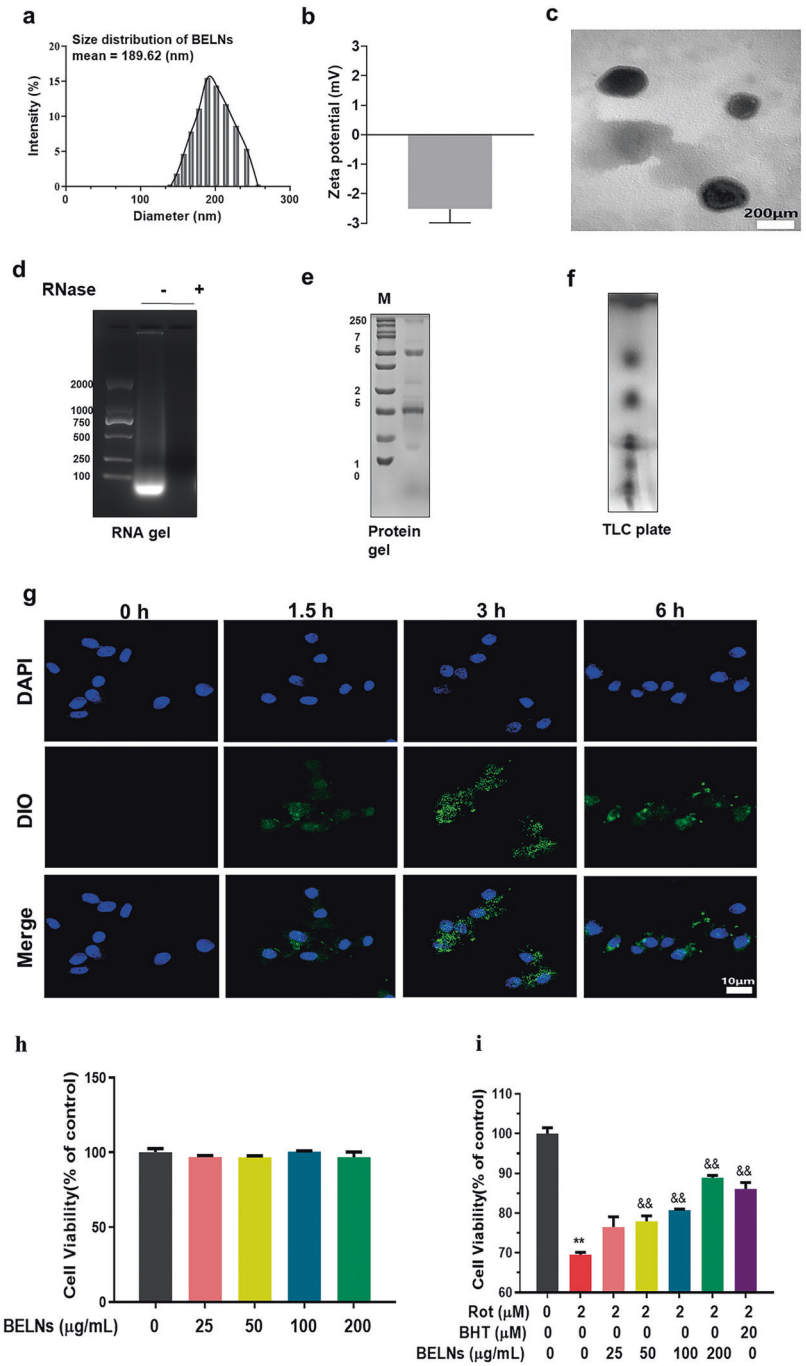

Fig. 1 Characterization of blueberry exosomes-like nanoparticles (BELNs). a Size distribution of the BELNs. **b** Surface zeta potential of the BELNs. **c** BELNs were visualized by transmission electron microscopy. **d** After the total RNA was extracted with a commercial RNA extraction kit, the RNA samples of the BELNs were pretreated without or with 10 μg/mL RNase for 30 min, and then, the RNA samples were separated by electrophoresis on a 3% agarose gel and visualized with a UVP imaging system. **e** The prteins (30 μg) of the BELNs were separated with 10% SDS-PAGE protein gels and detected with Coomassie Blue staining. **f** After the lipids were extracted from BELNs, they were separated on thin-layer chromatography (TLC) plate and developed by spraying the plate with a 10% copper sulfate and 8% phosphoric acid solution. **g** After HepG2 cells were incubated with DiO (green)-labeled BELNs for 0, 1.5, 3, or 6 h at 37 °C, the nuclei were labeled with DAPI staining (blue). The uptake of BELNs was observed and imaged by an E-C2 confocal microscope (Nikon, Tokyo, Japan). The scale bar = 10 μm. **h** After HepG2 cells were incubated with 0 (same volume of PBS), 25, 50, 100, and 200 μg/mL BELNs for 24 h, the cell viability was determined with MTT assays. Data are the mean ± SD ($n = 6$). **i** After HepG2 cells were preincubated with 0, 25, 50, 100, or 200 μg/mL BELNs or 20 μM BHT for 4 h, 2 μM rotenone was added and incubated for 24 h. Cell viability was determined using the MTT assay. BHT (20 μM) was used as a positive control in this study. Data are shown as the mean ± SD ($n = 6$). $^{**}P < 0.01$ vs. the solvent control (Con, PBS in this study), and $^{\&\&}P < 0.01$ vs. the rotenone alone group.

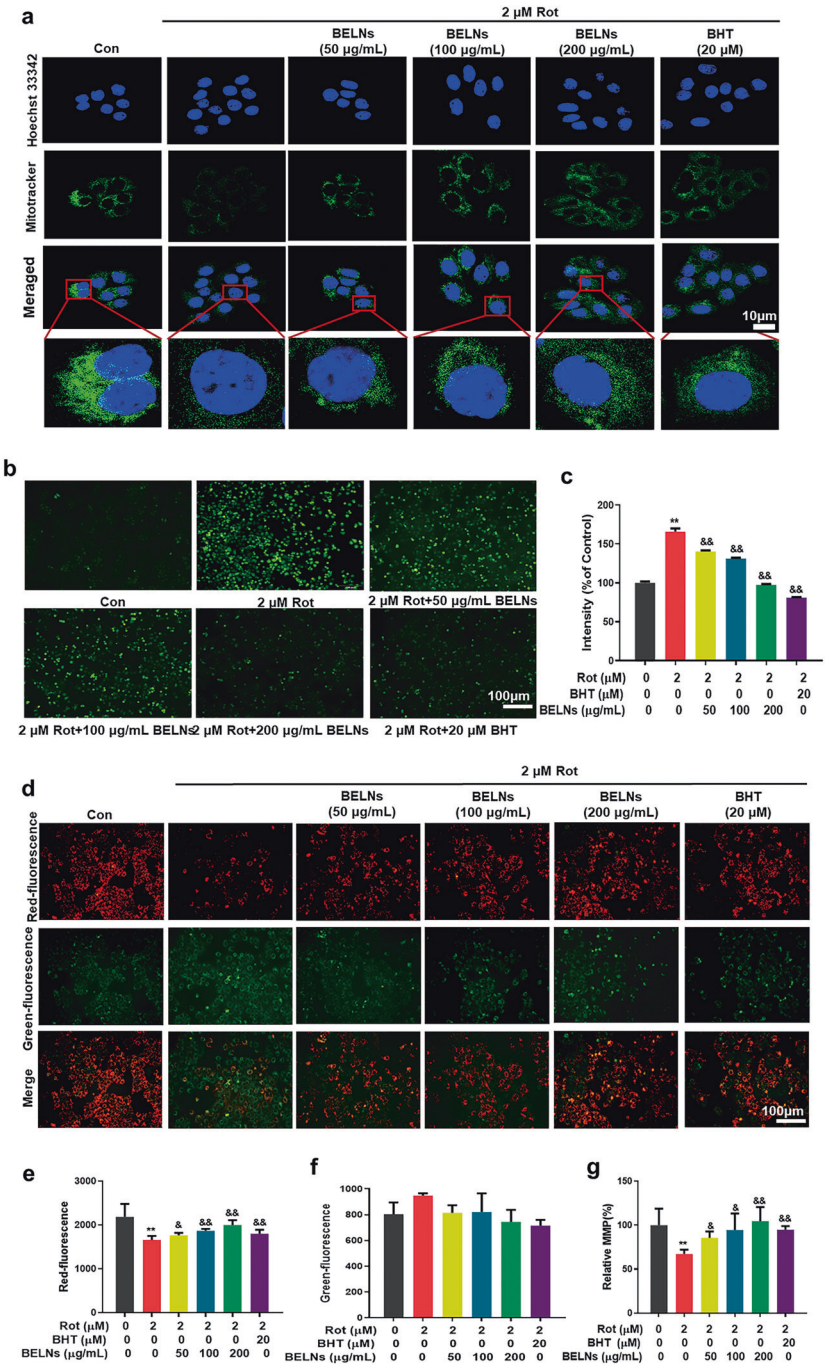

Fig. 2 BELNs prevented oxidative stress in the rotenone-treated HepG2 cells. a After HepG2 cells were preincubated with 50, 100, or 200 μg/mL BELNs or 20 μM BHT for 4 h, 2 μM rotenone was added and incubated for 24 h. The cells were stained with MitoTracker (Beyotime, Shanghai, China), and the nuclei were labeled with Hoechst 33342 (Beyotime, Shanghai, China). The content of mitochondria was observed and imaged by an E-C2 confocal microscope (Nikon, Tokyo, Japan). Scale bar = 10 μm. **b** and **c** After HepG2 cells were preincubated with 50, 100, or 200 μg/mL BELNs or 20 μM BHT for 4 h, 2 μM rotenone was added and incubated for 24 h. The cells were incubated with 25 μM CM-H2DCFDA in serum-free medium for 30 min at 37 °C and then washed once with PBS. The cells were imaged with fluorescence microscopy (Nikon, Tokyo, Japan), and the fluorescence intensity was determined with a microplate reader (Tecan, Sunrise, USA) with excitation at 485 nm and emission at 530 nm. Data are shown as the mean ± SD ($n = 8$). $^{**}P < 0.01$ vs. the control and $^{\&\&}P < 0.01$ vs. the rotenone alone group. Scale bar = 100 μm. After HepG2 cells were preincubated with 50, 100, or 200 μg/mL BELNs or 20 μM BHT for 4 h, 2 μM rotenone was added and incubated for 24 h. The cells were stained with 10 μg/mL JC-1 for 20 min at 37 °C. Monomeric JC-1 (green) and aggregated JC-1 (red) were imaged with a fluorescence microscope (Nikon, Tokyo, Japan) at Ex/Em = 514 nm/529 nm (green) or 585 nm/590 nm (red), respectively (**d**). Similarly, the fluorescence intensity was determined with a microplate reader (Sunrise, Tecan, CA, USA) for aggregated JC-1 (**e**) or monomeric JC-1 (**f**), and the relative mitochondrial membrane potential (MMP) was calculated (**g**). Data are shown as the mean ± SD ($n = 6$). $^{**}P < 0.01$ vs. the solvent control (Con, PBS in this study), $^{\&}P < 0.05$, and $^{\&\&}P < 0.01$ vs. the rotenone alone group. Scale bar = 100 μm.

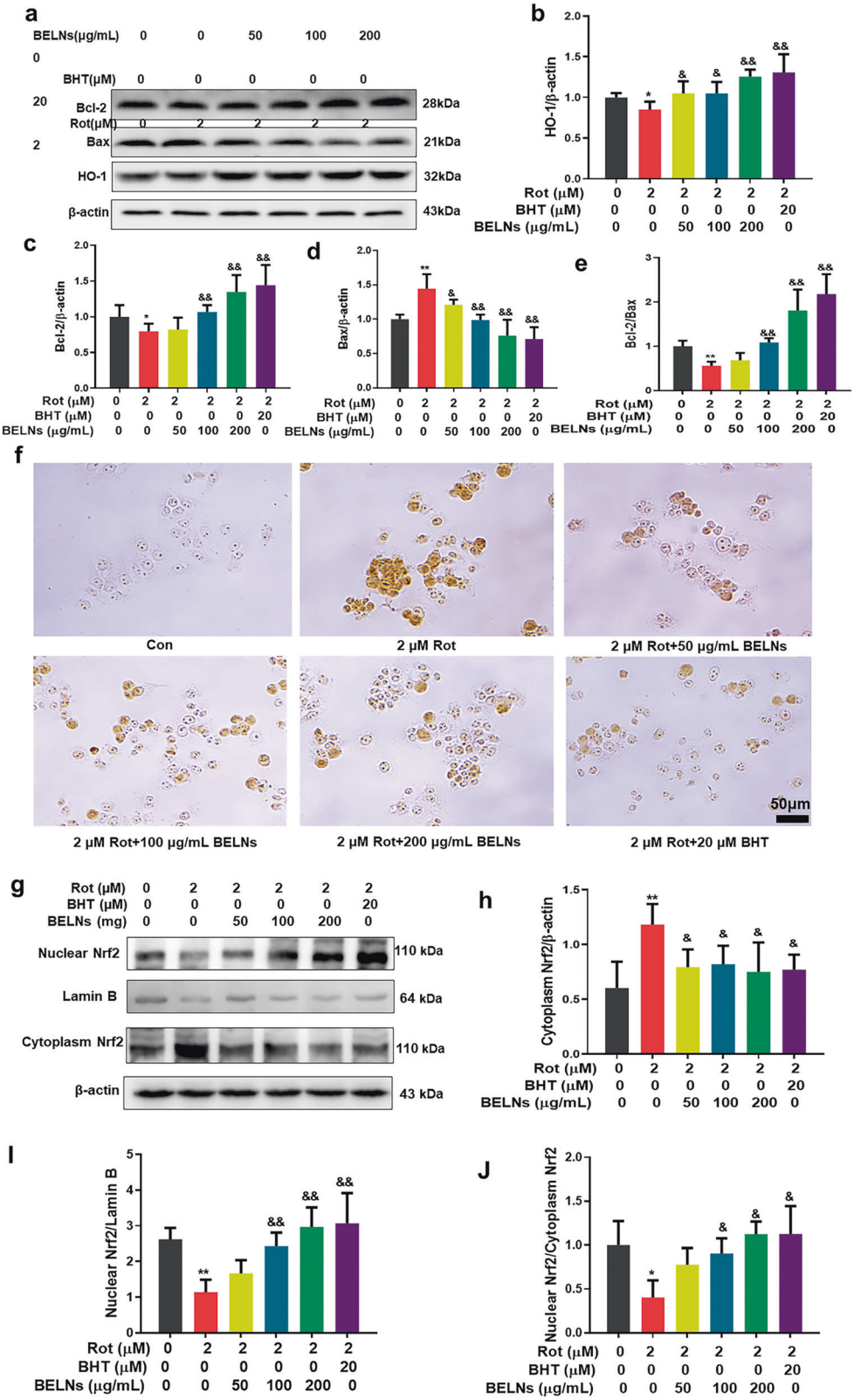

Fig. 3 BELNs attenuated cell apoptosis induced by rotenone in HepG2 cells. After HepG2 cells were preincubated with 50, 100, or 200 μg/mL BELNs or 20 μM BHT for 4 h, 2 μM rotenone was added and incubated for 24 h. Apoptosis-associated proteins (**a**), including HO-1 (**b**), Bcl-2 (**c**) and Bax (**d**), were assessed by Western blotting, and the ratio of Bcl-2/Bax was calculated (**e**). Apoptotic cells were stained with TUNEL (**f**) according to the procedure introduced in the "Materials and methods". **g**–**j** The protein level of Nrf2 in the cytoplasm and nucleus was determined by Western blots. Data are expressed as the mean ± SD from at least three independent experiments. $^{*}P < 0.05$ and $^{**}P < 0.01$ vs. the control and $^{\&}P < 0.05$ and $^{\&\&}P < 0.01$ vs. the rotenone alone group. Scale bar = 50 μm.

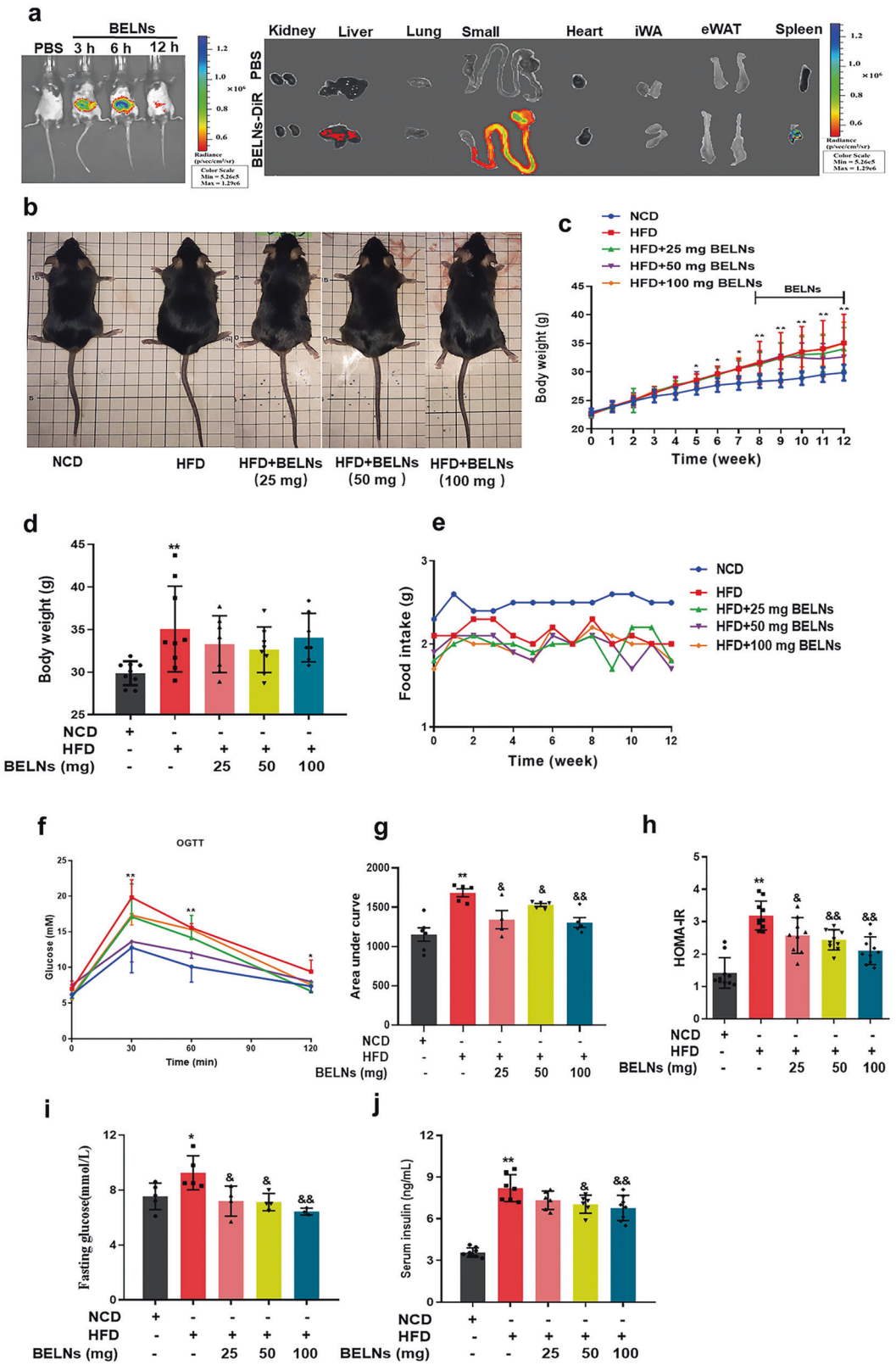

Fig. 4 BELNs improved insulin resistance and decreased fasting glucose and insulin content in the HFD-fed mice. a After DIR-labeled BELNs were administered intragastrically, the mice were observed and imaged with an IVIS Spectrum In Vivo Imaging system (PerkinElmer, CA, USA) at 0, 3, 6, and 12 h, and the distribution of BELNs in the kidney, liver, lung, small intestine, heart iWAT, eWAT, and spleen was identified at 3 h. **b**–**j** After C57BL/6 mice were fed an HFD (D12451, Research Diets) for 8 weeks, they were intragastrically administered 25, 50, and 100 mg/mouse BELNs (once every other day, intragastrically) for 4 weeks. Body weight (**c** and **d**) and food intake (**e**) were monitored every other day, and the glucose tolerance (**f**), fasting blood glucose (**i**), and insulin content in serum (**j**) were measured. The area under the curve (AUC, **g**) and homeostasis model assessment of insulin resistance (HOMA-IR) (**h**) were calculated. Data are the mean ± SD ($n = 5$-8). $^{*}P < 0.05$ and $^{**}P < 0.01$ vs. the NCD (normal chow diet) group; $^{\&}P < 0.05$ and $^{\&\&}P < 0.01$ vs. the HFD alone group.

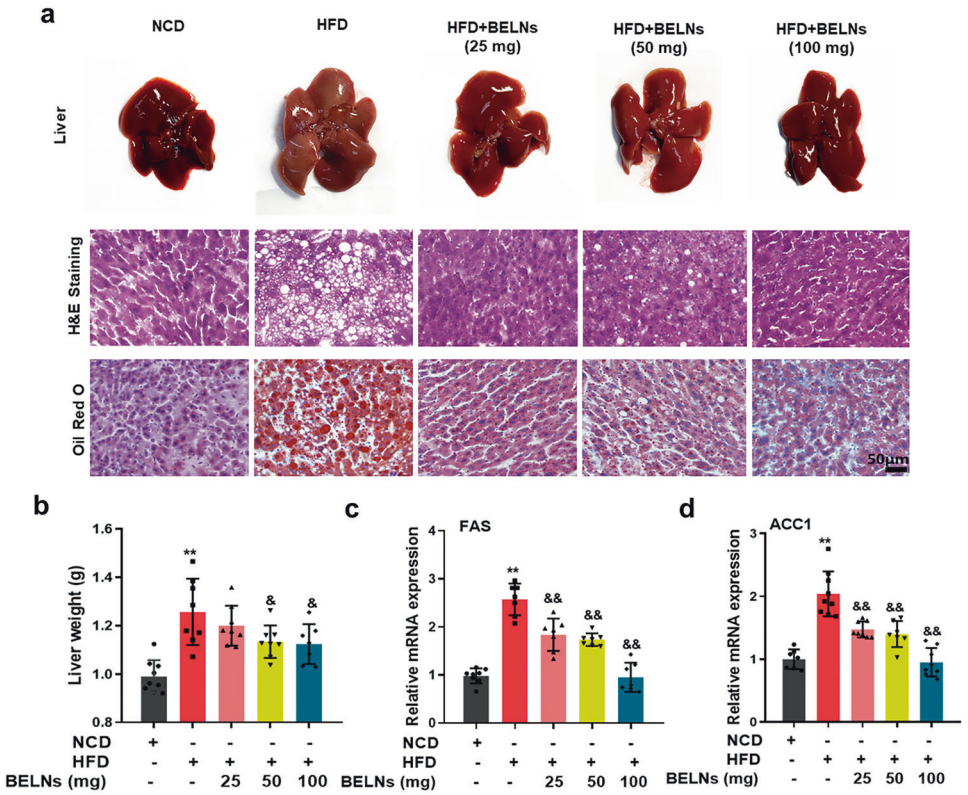

Fig. 5 BELNs prevented vacuoles and the accumulation of lipid droplets and decreased the expression of fatty acid synthases in hepatocytes in the HFD-fed mice. After the HFD-fed mice were administered 25, 50, and 100 mg/mouse BELNs (administered intragastrically) for 4 weeks, the liver sections were stained with H&E and oil red O (**a**), the liver weight was measured (**b**) ($n = 5$–8), and the mRNA levels of FAS (**c**) and ACC1 (**d**) were determined by qRT-PCR. Data are shown as the mean ± SD ($n = 6$). $^{**}P < 0.01$ vs. the NCD (normal chow diet) group and $^{\&}P < 0.05$ and $^{\&\&}P < 0.01$ vs. the HFD group. Scale bar = 50 μm.

mice administered BELNs for 4 weeks. The results indicated that the HFD significantly decreased the activities of SOD and GSH, two important antioxidative enzymes, and increased the content of MDA in the liver of the HFD-fed mice, but administration of the BELNs for 4 weeks prevented the effect of the HFD in a dose-dependent manner in C57BL/6 mice (Fig. 7a–c).

We also determined the expression of Bcl-2, Bax, and HO-1 in the BELN-administered HFD-fed mice. Western blot data demonstrated that the HFD reduced the protein levels of Bcl-2 and HO-1 and increased the protein level of Bax, but administration of the BELNs for 4 weeks prevented the effects of the HFD on the expression of Bcl-2, Bax, and HO-1 in the livers of C57BL/6 mice (Fig. 7d–h).

In chronic liver diseases, oxidative stress may contribute to the progression of liver injury, fibrosis, and carcinogenesis, and Nrf2 is the key regulator of cellular redox balance in hepatocytes [30]. In this study, we determined the distribution of Nrf2 in the hepatocytes of the HFD-fed mice. The Western blot results showed that the HFD induced a slight increase in Nrf2 in the cytoplasm, but BELN supplementation accelerated the translocation of Nrf2 from the cytoplasm to nuclei in the liver of the HFD-fed mice (Fig. 8a–d). The immunochemistry results further confirmed the effect of BELNs on the distribution of Nrf2 in the livers of the HFD-fed mice (Fig. 8e).

DISCUSSION

NAFLD is the major cause of chronic liver diseases and represents a wide spectrum of liver disorders in most parts of the world [31, 32]. Given that the liver is a key regulator of whole-body energy homeostasis, it is not surprising that many individuals with NAFLD also show metabolic complications, including insulin resistance, cardiovascular disease, and type 2 diabetes mellitus [32]. Emerging evidence indicates that although genetic predisposition and sedentary lifestyle have been identified to be associated with NAFLD, mitochondrial dysfunction is now widely accepted to play a central role in the pathogenesis and progression of this disease [33, 34]. Unfortunately, no drugs have been approved to treat NAFLD by the U.S. Food and Drug Administration. Currently, the first step in the management of NAFLD in most patients is the implementation of lifestyle modifications that focus on healthy eating habits and regular exercise, but regrettably, meaningful lifestyle modification is difficult to achieve and sustain for most people [35, 36]. Several studies have shown that supplementation with antioxidants is beneficial for NAFLD [37]. Recently, researchers have focused on edible plant-derived nanoparticles that display interspecies communication and their nutraceutical and pharmacological properties, including anti-inflammatory and antioxidative functions. It has been reported that grape-derived exosome-like nanoparticles can modulate the remodeling of intestinal tissues by triggering stem cell proliferation in the intestinal epithelium and preventing colitis induced by dextran sulfate sodium [38], and ginger-derived exosome-like nanoparticles play a pivotal role in the activation of Nrf2 in a TLR4/TRIF-dependent manner to protect against alcohol-induced liver damage [39]. In the current study, our data revealed that BELNs were one kind of novel component in blueberry that showed antioxidative effects in rotenone-induced HepG2 cells and in the liver of HFD-fed mice, suggesting that BELNs might be beneficial in the treatment of NAFLD due to their antioxidative activity.

Hepatocytes are rich in mitochondria. It has been reported that 2% of oxygen is transformed into ROS by mitochondria under basal conditions in hepatocytes [40, 41]. At mitochondrial

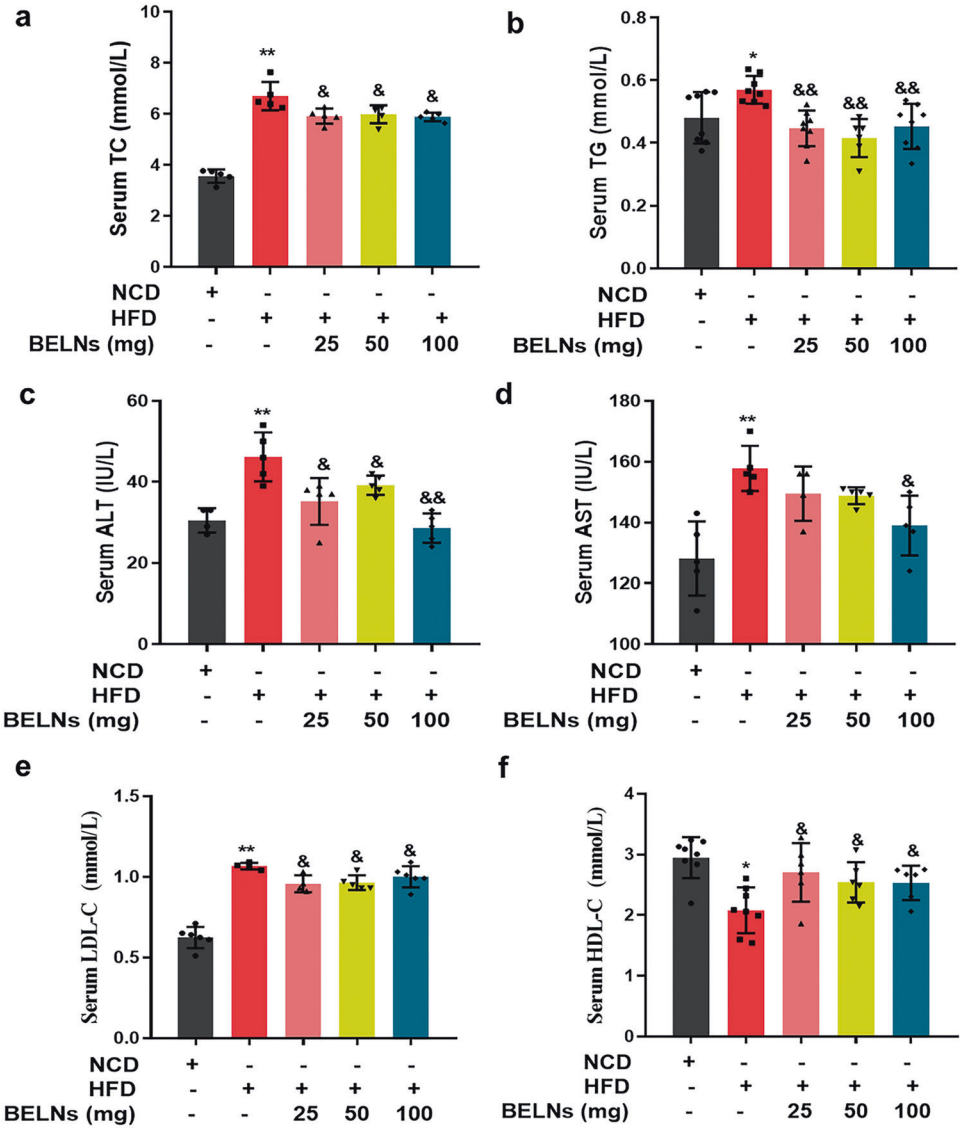

Fig. 6 BELNs improved liver dysfunction in the HFD-fed mice. After the HFD-fed mice were administered 25, 50, and 100 mg/mouse BELNs (administered intragastrically) for 4 weeks, the TC (**a**), TG (**b**), ALT (**c**), AST (**d**), LDL-C (**e**), and HDL-C levels (**f**) in serum were measured with commercial kits according to the suggestions from the suppliers. Data are shown as the mean ± SD ($n = 5$-8). $^{*}P < 0.05$ and $^{**}P < 0.01$ vs. the NCD (normal chow diet) group; $^{\&}P < 0.05$ and $^{\&\&}P < 0.01$ vs. the HFD group.

complexes I and III, electrons can prematurely escape and interact with oxygen molecules, thus resulting in the production of ROS. Excessive ROS production is one of the major mechanisms of mitochondrial dysfunction, which can cause lipid peroxidation and damage to mitochondrial DNA and the membrane [40, 42]. In this study, our data indicated that preincubation with the BELNs attenuated the production of ROS, increased the content of mitochondria and the mitochondrial membrane potential, and prevented cell apoptosis by regulating the expression of Bcl-2, Bax, and HO-1 in the rotenone-treated HepG2 cells. Moreover, we observed that BELN supplementation effectively reduced MDA content, increased the activities of SOD and GSH, enhanced the expression of the Bcl-2 and HO-1 proteins, and reduced the protein level of Bax in the livers of the HFD-fed mice. All these findings suggested that BELNs could be useful for the treatment of NAFLD due to their antioxidative and antiapoptotic activities.

Under conditions of redox imbalance, Nrf2 has been reported to be activated to induce the expression of detoxifying/antioxidative genes to remodel cell metabolism and maintain redox homeostasis in hepatocytes [43]. Nrf2 is a key transcription factor that regulates the expression of multiple antioxidative enzymes, such as HO-1, NAD(P)H:quinone oxidoreductase 1 (NQO1), SOD, GPx, and CAT [44, 45]. Therefore, modulation of the Nrf2 signaling pathway has been considered to be therapeutically important in preventing oxidative stress-induced damage in mammalian cells. In this study, we further investigated the antioxidant mechanism of BELNs in hepatocytes. The results indicated that the translocation of Nrf2 from the cytoplasm to the nucleus was potentiated in the BELN-treated HepG2 cells and the livers of the HFD-fed mice supplemented with the BELNs. The results of the present study suggested that the antioxidative activity of BELNs could benefit from the modulation of Nrf2 distribution to induce the expression of antioxidative proteins and antioxidative enzymes.

The liver is the key regulator of systemic lipid metabolism in mammalian cells. In addition to β-oxidation for energy production, fatty acids can be esterified to predominantly produce triacylglycerol and stored within lipid droplets in the liver [46]. One important source of fatty acids is from nonlipid precursors by de

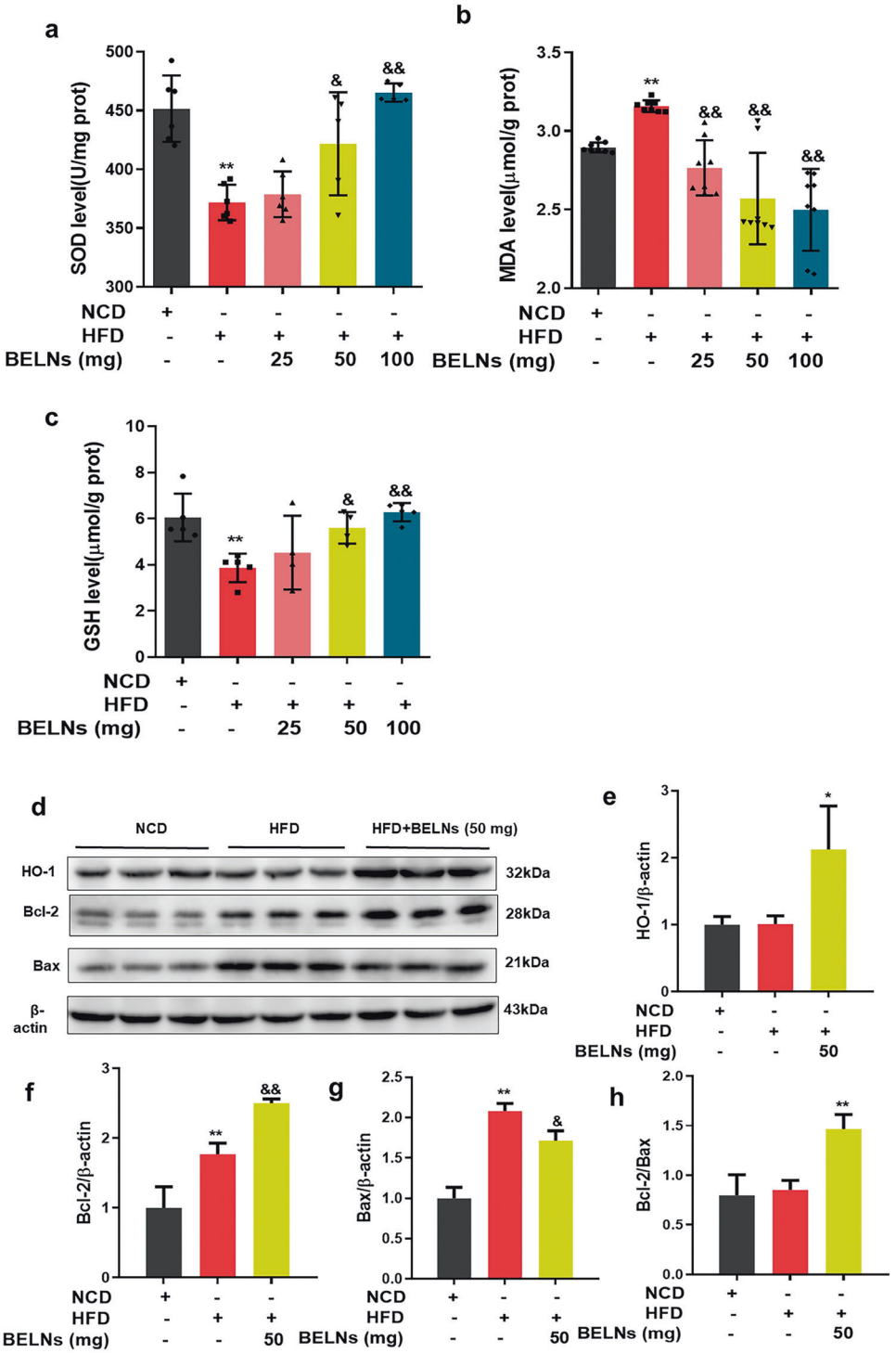

Fig. 7 BELNs regulated the levels of redox-associated proteins in the HFD-fed mice. After the HFD-fed mice were administered 25, 50, and 100 mg/mouse BELNs (administered intragastrically) for 4 weeks, the activities of SOD (**a**), GSH (**b**), and MDA (**c**) were measured with commercial kits according to the suggestions from the suppliers. Data are presented as the mean ± SD ($n = 6$). $^{**}P < 0.01$ vs. the NCD (normal chow diet) group and $^{\&}P < 0.05$ and $^{\&\&}P < 0.01$ vs. the HFD alone group. **d–h** The protein levels of HO-1, Bcl-2, and Bax were determined by Western blotting, and the ratio of Bcl-2/Bax was calculated. Data are shown as the mean ± SD ($n = 3$). $^{*}P<0.05$, $^{**}P<0.01$ vs NCD group. $^{\&}P < 0.05$ and $^{\&\&}P < 0.01$ vs. the HFD alone group.

novo lipogenesis, which occurs via transcriptional regulation of acetyl-CoA carboxylase 1 (ACC1) and FAS, primarily through sterol regulatory element-binding protein 1c and carbohydrate-responsive element-binding protein [47]. Therefore, one approach to treat NAFLD is to reduce the endogenous production of fatty acids in the liver by inhibiting de novo lipogenesis [48, 49]. Here, our data revealed that in addition to improving liver dysfunction by decreasing the activities of AST and ALT, BELN supplementation also attenuated the accumulation of lipid droplets and reduced the expression of FAS and ACC1 in the livers of the

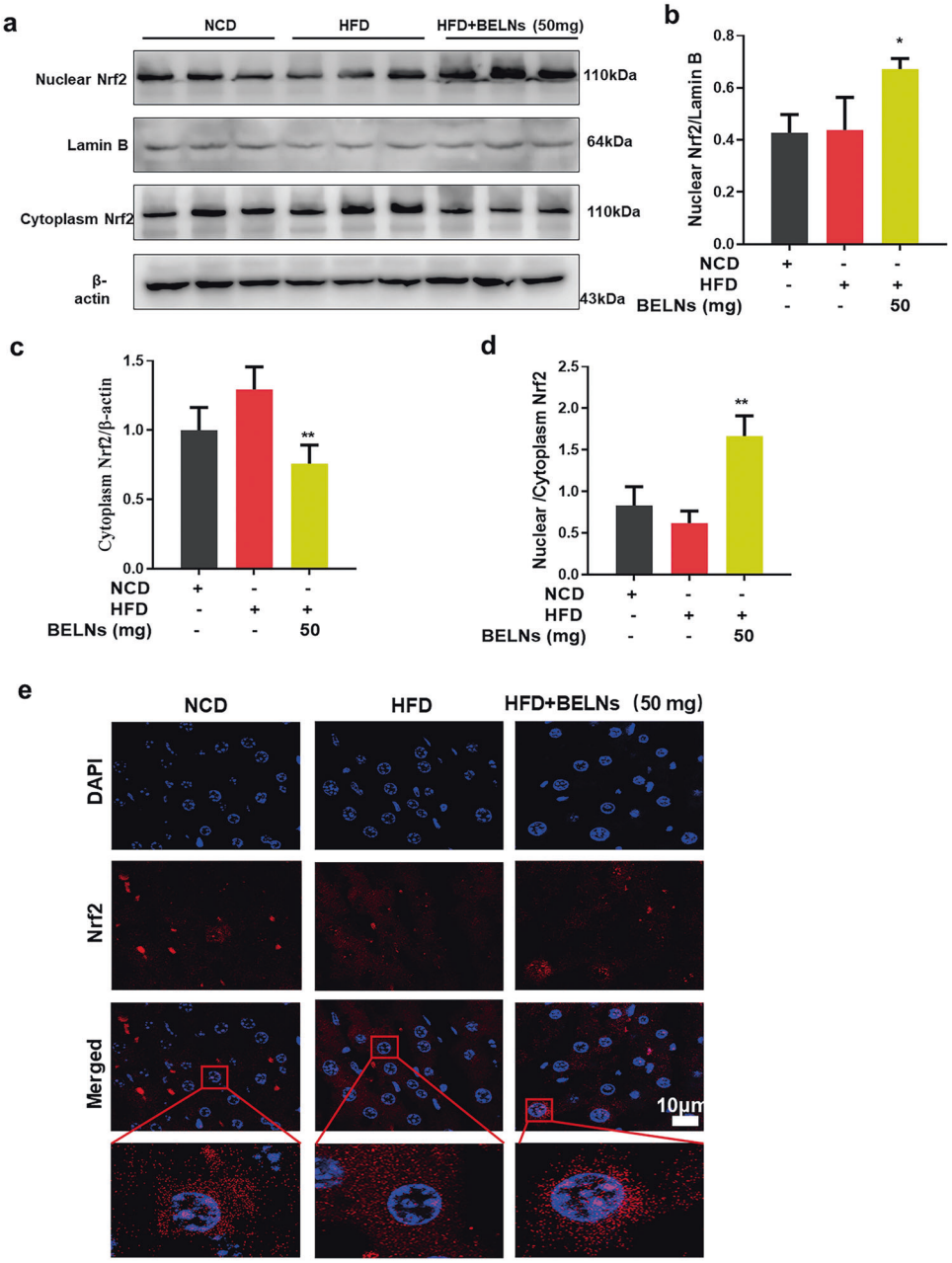

Fig. 8 BELNs regulated the distribution of Nrf2 in the livers of the HFD-fed mice. After the HFD-fed mice were administered 25, 50, and 100 mg/mouse BELNs (administered intragastrically) for 4 weeks, the protein level of Nrf2 in the nuclei (**a**, **b**) and cytoplasm (**a**, **c**) of liver tissue was determined by Western blotting. The ratio of nuclear/cytoplasm Nrf2 was calculated (**d**). The immunochemistry analysis of distribution of Nrf2 in the livers of the HFD-fed mice (**e**). Data are expressed as the mean ± SD ($n = 3$). *$P < 0.05$ and *$P < 0.01$ vs. the HFD alone group. Scale bar = 100 μm.

HFD-fed mice. This finding suggests that BELNs might improve NAFLD by their effects on de novo lipogenesis.

Exosomes are small membranous nanoparticles that can be formed and secreted into the extracellular environment by a variety of mammalian cells [50–52]. Increasing evidence indicates that similar to exosomes secreted by mammalian cells, edible plant-derived exosome-like nanoparticles can serve as extracellular messengers to mediate cell-cell communication and even function in interspecies communication through their cargos, such as miRNAs, bioactive lipids, and proteins [53]. Therefore, given the proper origin and cargo, plant-derived edible nanoparticles could be used as natural therapeutics against a variety of diseases. In this study, we isolated BELNs and showed that they contained RNA, proteins, and lipids, which could be taken up by HepG2 cells and C57BL/6 mice and rapidly penetrate the intestinal mucus barrier into the liver and spleen. Our data revealed that the BELNs showed antioxidative effects and could prevent cell apoptosis in the rotenone-treated HepG2 cells and in the livers of the HFD-fed mice.

A growing body of evidence reveals that insulin resistance, as an important risk factor, is involved in the pathogenesis of NAFLD by increasing de novo lipogenesis and impairing lipolysis in adipose tissue, consequently increasing accumulation of hepatic fat, and NAFLD is strongly associated with insulin resistance as

well as reduced whole-body insulin sensitivity [54, 55]. In the current study, BELN supplementation was shown to improve insulin resistance and liver dysfunction by reducing the expression of genes associated with de novo lipogenesis in the livers of the HFD-fed mice, suggesting that BELNs may possess intrinsic therapeutic activity against NAFLD by improving insulin resistance.

Taken together with our current data, these findings indicate that BELNs could reduce the cell apoptosis induced by rotenone in HepG2 cells through their antioxidative activity, improve insulin resistance and liver dysfunction by decreasing the levels of AST and ALT, and attenuate the accumulation of lipid droplets by inhibiting the expression of FAS and ACC1, the two key transcription factors for de novo lipogenesis in the liver of the HFD-fed mice. All these findings indicate that BELNs can be used as a novel antioxidant for the treatment of NAFLD.

ACKNOWLEDGEMENTS

This work was supported by grants from the National Natural Science Foundation of China (81803800), the Chongqing Science and Technology Committee (2017jcyjB0077), and the Innovative Research Team Development Program at the University of Chongqing (CXTDX201601031). The authors are grateful to Prof. Junzeng Zhang from the National Research Council of Canada for his review of the original draft.

AUTHOR CONTRIBUTIONS

WJZ, YPB, and QHW performed the experiments; LY and YLZ analyzed the data. JHL and FY were the major contributors to designing the research and writing the manuscript. All authors read and approved the final manuscript.

ADDITIONAL INFORMATION

Supplementary information The online version contains supplementary material available at https://doi.org/10.1038/s41401-021-00681-w.

Competing interests: The authors declare no competing interests.

REFERENCES

1. Pearlman B. How would you manage this patient with nonalcoholic fatty liver disease? Ann Intern Med. 2019;171:861–2.
2. Angulo P. Nonalcoholic fatty liver disease. Rev Gastroenterol Mex. 2005;70(Suppl 3):52–6.
3. Baran B, Akyuz F. Non-alcoholic fatty liver disease: what has changed in the treatment since the beginning? World J Gastroenterol. 2014;20:14219–29.
4. Yamaguchi K, Yang L, McCall S, Huang J, Yu XX, Pandey SK, et al. Inhibiting triglyceride synthesis improves hepatic steatosis but exacerbates liver damage and fibrosis in obese mice with nonalcoholic steatohepatitis. Hepatology. 2007;45:1366–74.
5. Begriche K, Massart J, Robin MA, Bonnet F, Fromenty B. Mitochondrial adaptations and dysfunctions in nonalcoholic fatty liver disease. Hepatology. 2013;58:1497–507.
6. Albano E, Mottaran E, Vidali M, Reale E, Saksena S, Occhino G, et al. Immune response towards lipid peroxidation products as a predictor of progression of non-alcoholic fatty liver disease to advanced fibrosis. Gut. 2005;54:987–93.
7. Gariani K, Ryu D, Menzies K, Yi H, Stein S, Zhang H, et al. Inhibiting poly ADP-ribosylation increases fatty acid oxidation and protects against fatty liver disease. J Hepatol. 2017;66:132–41.
8. Borrelli A, Bonelli P, Tuccillo FM, Goldfine ID, Evans JL, Buonaguro FM, et al. Role of gut microbiota and oxidative stress in the progression of non-alcoholic fatty liver disease to hepatocarcinoma: current and innovative therapeutic approaches. Redox Biol. 2018;15:467–79.
9. Damba T, Bourgonje AR, Abdulle AE, Pasch A, Sydor S, van den Berg EH, et al. Oxidative stress is associated with suspected non-alcoholic fatty liver disease and all-cause mortality in the general population. Liver Int. 2020;40:2148–59.
10. Yamada T, Murata D, Adachi Y, Itoh K, Kameoka S, Igarashi A, et al. Mitochondrial stasis reveals p62-mediated ubiquitination in Parkin-independent mitophagy and mitigates nonalcoholic fatty liver disease. Cell Metab. 2018;28:588–604. e5.
11. Dornas W, Schuppan D. Mitochondrial oxidative injury: a key player in nonalcoholic fatty liver disease. Am J Physiol Gastrointest Liver Physiol. 2020;319:G400–G11.
12. Wang L, Liu X, Nie J, Zhang J, Kimball SR, Zhang H, et al. ALCAT1 controls mitochondrial etiology of fatty liver diseases, linking defective mitophagy to steatosis. Hepatology. 2015;61:486–96.
13. Whyte AR, Rahman S, Bell L, Edirisinghe I, Krikorian R, Williams CM, et al. Improved metabolic function and cognitive performance in middle-aged adults following a single dose of wild blueberry. Eur J Nutr. 2021;60:1521–36. https://doi.org/10.1007/s00394-020-02336-8.
14. Wu T, Gao Y, Guo X, Zhang M, Gong L. Blackberry and blueberry anthocyanin supplementation counteract high-fat-diet-induced obesity by alleviating oxidative stress and inflammation and accelerating energy expenditure. Oxid Med Cell Longev. 2018;2018:4051232.
15. Xu N, Meng H, Liu T, Feng Y, Qi Y, Zhang D, et al. Blueberry phenolics reduce gastrointestinal infection of patients with cerebral venous thrombosis by improving depressant-induced autoimmune disorder via miR-155-mediated brain-derived neurotrophic factor. Front Pharmacol. 2017;8:853.
16. Zepeda A, Aguayo LG, Fuentealba J, Figueroa C, Acevedo A, Salgado P, et al. Blueberry extracts protect testis from hypobaric hypoxia induced oxidative stress in rats. Oxid Med Cell Longev. 2012;2012:975870.
17. Zhuge Q, Zhang Y, Liu B, Wu M. Blueberry polyphenols play a preventive effect on alcoholic fatty liver disease C57BL/6 J mice by promoting autophagy to accelerate lipolysis to eliminate excessive TG accumulation in hepatocytes. Ann. Palliat Med. 2020;9:1045–54.
18. Wang Y, Cheng M, Zhang B, Nie F, Jiang HJPo. Dietary supplementation of blueberry juice enhances hepatic expression of metallothionein and attenuates liver fibrosis in rats. PLoS One. 2013;8:e58659.
19. Wang YP, Cheng ML, Zhang BF, Mu M, Wu J. Effects of blueberry on hepatic fibrosis and transcription factor Nrf2 in rats. World J Gastroenterol. 2010;16:2657–63.
20. Kalluri R, LeBleu V. The biology function and biomedical applications of exosomes. Science. 2020;367:640–55.
21. Mathieu M, Martin-Jaular L, Lavieu G, Théry C. Specificities of secretion and uptake of exosomes and other extracellular vesicles for cell-to-cell communication. Nat Cell Biol. 2019;21:9–17.
22. Folch J, Lees M, Sloane, Stanley GH. A simple method for the isolation and purification of total lipids from animal tissues. J Biol Chem. 1957;226:497–509.
23. Liu XR, Cao L, Li T, Chen LL, Yu YY, Huang WJ, et al. Propofol attenuates H2O2-induced oxidative stress and apoptosis via the mitochondria- and ER-medicated pathways in neonatal rat cardiomyocytes. Apoptosis. 2017;22:639–46.
24. Yang J, Song X, Feng Y, Liu N, Fu Z, Wu J, et al. Natural ingredients-derived antioxidants attenuate H_2O_2-induced oxidative stress and have chondroprotective effects on human osteoarthritic chondrocytes via Keap1/Nrf2 pathway. Free Radic Biol Med. 2020;152:854–64.
25. Siddiqui MA, Ahmad J, Farshori NN, Saquib Q, Jahan S, Kashyap MP, et al. Rotenone-induced oxidative stress and apoptosis in human liver HepG2 cells. Mol Cell Biochem. 2013;384:59–69.
26. Gandham S, Su X, Wood J, Nocera A, Alli S, Milane L, et al. Technologies and standardization in research on extracellular vesicles. Trends Biotechnol. 2020;38:1066–98.
27. Niu Y, Zhou W, Nie Z, Shin K, Cui X. Melatonin enhances mitochondrial biogenesis and protects against rotenone-induced mitochondrial deficiency in early porcine embryos. J Pineal Res. 2020;68:e12627.
28. Cox C, McKay S, Holmbeck M, Christian B, Scortea A, Tsay A, et al. Mitohormesis in mice via sustained basal activation of mitochondrial and antioxidant signaling. Cell Metab. 2018;28:776–86. e5.
29. Garcia-Ruiz C, Fernandez-Checa JC. Mitochondrial oxidative stress and antioxidants balance in fatty liver disease. Hepatol Commun. 2018;2:1425–39.
30. Mohs A, Otto T, Schneider K, Peltzer M, Boekschoten M, Holland C, et al. Hepatocyte-specific NRF2 activation controls fibrogenesis and carcinogenesis in steatohepatitis. J Hepatol. 2021;74:638–48.
31. Wang X, Malhi H. Nonalcoholic fatty liver disease. Ann Intern Med. 2018;169:ITC65–ITC80.
32. Rinella M. Nonalcoholic fatty liver disease: a systematic review. JAMA. 2015;313:2263–73.
33. Sanyal A. Past, present and future perspectives in nonalcoholic fatty liver disease. Nat Rev Gastroenterol Hepatol. 2019;16:377–86.
34. Satapati S, Kucejova B, Duarte J, Fletcher J, Reynolds L, Sunny N, et al. Mitochondrial metabolism mediates oxidative stress and inflammation in fatty liver. J Clin Invest. 2015;125:4447–62.
35. Bellentani S, Dalle Grave R, Suppini A, Marchesini G, Fatty Liver Italian N. Behavior therapy for nonalcoholic fatty liver disease: the need for a multidisciplinary approach. Hepatology. 2008;47:746–54.

36. Centis E, Marzocchi R, Di Domizio S, Ciaravella MF, Marchesini G. The effect of lifestyle changes in non-alcoholic fatty liver disease. Dig Dis. 2010;28:267–73.
37. Paul S, Davis A. Diagnosis and management of nonalcoholic fatty liver disease. JAMA. 2018;320:2474–5.
38. Ju S, Mu J, Dokland T, Zhuang X, Wang Q, Jiang H, et al. Grape exosome-like nanoparticles induce intestinal stem cells and protect mice from DSS-induced colitis. Mol Ther. 2013;21:1345–57.
39. Zhuang X, Deng ZB, Mu J, Zhang L, Yan J, Miller D, et al. Ginger-derived nanoparticles protect against alcohol-induced liver damage. J Extracell Vesicles. 2015;4:28713.
40. Mansouri A, Gattolliat C, Asselah T. Mitochondrial dysfunction and signaling in chronic liver diseases. Gastroenterology. 2018;155:629–47.
41. Mantena SK, King AL, Andringa KK, Eccleston HB, Bailey SM. Mitochondrial dysfunction and oxidative stress in the pathogenesis of alcohol- and obesity-induced fatty liver diseases. Free Radic Biol Med. 2008;44:1259–72.
42. Koek GH, Liedorp PR, Bast A. The role of oxidative stress in non-alcoholic steatohepatitis. Clin Chim Acta. 2011;412:1297–305.
43. Sies H, Jones D. Reactive oxygen species (ROS) as pleiotropic physiological signalling agents. Nat Rev Mol cell Biol. 2020;21:363–83.
44. Li M, Yu H, Pan H, Zhou X, Ruan Q, Kong D, et al. Nrf2 suppression delays diabetic wound healing through sustained oxidative stress and inflammation. Front Pharmacol. 2019;10:1099.
45. Zhao Y, Kong GY, Pei WM, Zhou B, Zhang QQ, Pan BB. Dexmedetomidine alleviates hepatic injury via the inhibition of oxidative stress and activation of the Nrf2/HO-1 signaling pathway. Eur Cytokine Netw. 2019;30:88–97.
46. Mashek D. Hepatic lipid droplets: a balancing act between energy storage and metabolic dysfunction in NAFLD. Mol Metab. 2020;101115. https://doi.org/10.1016/j.molmet.2020.101115.
47. Beaven S, Matveyenko A, Wroblewski K, Chao L, Wilpitz D, Hsu T, et al. Reciprocal regulation of hepatic and adipose lipogenesis by liver X receptors in obesity and insulin resistance. Cell Metab. 2013;18:106–17.
48. Samuel V, Shulman G. Nonalcoholic fatty liver disease as a nexus of metabolic and hepatic diseases. Cell Metab. 2018;27:22–41.
49. Hodson L, Gunn P. The regulation of hepatic fatty acid synthesis and partitioning: the effect of nutritional state. Nat Rev Endocrinol. 2019;15:689–700.
50. O'Brien K, Breyne K, Ughetto S, Laurent L, Breakefield X. RNA delivery by extracellular vesicles in mammalian cells and its applications. Nat Rev Mol Cell Biol. 2020;21:585–606.
51. Sato K, Meng F, Glaser S, Alpini G. Exosomes in liver pathology. J Hepatol. 2016;65:213–21.
52. Mittelbrunn M, Sánchez-Madrid F. Intercellular communication: diverse structures for exchange of genetic information. Nat Rev Mol Cell Biol. 2012;13:328–35.
53. Zheng J, Sharp S, Imamura F, Chowdhury R, Gundersen T, Steur M, et al. Association of plasma biomarkers of fruit and vegetable intake with incident type 2 diabetes: EPIC-InterAct case-cohort study in eight European countries. BMJ. 2020;370:m2194.
54. Kojta I, Chacinska M, Blachnio-Zabielska A. Obesity, bioactive lipids, and adipose tissue inflammation in insulin resistance. Nutrients. 2020;12:1305. https://doi.org/10.3390/nu12051305.
55. Dali-Youcef N, Mecili M, Ricci R, Andres E. Metabolic inflammation: connecting obesity and insulin resistance. Ann Med. 2013;45:242–53.